JOURNAL OF GEOPHYSICAL RESEARCH, VOL. 106, NO. C3, PAGES 4449–4462, MARCH 15, 2001

Interannual variability of summer sea ice thickness in the Siberian and central Arctic under different atmospheric circulation regimes

Christian Haas

Alfred Wegener Institute, Bremerhaven, Germany

Hajo Eicken

Geophysical Institute, University of Alaska Fairbanks, Fairbanks, Alaska

Abstract. Extensive drill hole and electromagnetic induction measurements of sea ice thickness in the Siberian and central Arctic Seas in the summers of 1993, 1995, and 1996 reveal significant interannual variability. In the Laptev Sea, minimum and maximum modal first-year ice thicknesses amounted to 1.25 and 1.85 m in 1995 and 1996, respectively. Ice thickness correlates with ice extent, which reached a record minimum in August 1995 and was well above average in 1996. These differences are explained by the strength and location of a summer cyclonic atmospheric circulation pattern affecting both ice advection and surface melt. From drifting buoys deployed in 1995 and satellite radar backscatter data, first- and second-year ice regimes are delineated. Differences in first-year ice backscatter coefficients between 1993, 1995, and 1996 are explained by differences in level ice surface roughness. The Lagrangian evolution of ice thickness between 1995 and 1996 is studied. While the shape of the thickness distribution does not change significantly, the mean (modal) ice thickness of the ice field increases from 1.80 m (1.25 m) in 1995 to 2.86 m (2.25 m) in 1996. The thickness distribution of second-year ice in 1996 closely agrees with that of level multiyear ice downstream in the Transpolar Drift obtained in 1991. In 1996, mean level ice thickness increases at 0.23 and 0.16 m deg^{-1} with latitude in the Kara and Laptev Sea sectors of the Arctic Ocean, respectively.

1. Introduction

The Laptev and East Siberian Seas are the main source regions for sea ice that is transported across the Arctic Ocean toward Fram Strait by the Transpolar Drift [*Gordienko,* 1958; *Colony and Thorndike,* 1984; *Harder et al.,* 1998; *Rigor and Colony,* 1997]. Therefore ice formation and decay in these waters are of fundamental importance for the sea ice budget in the Arctic and for basinwide ocean-ice-atmosphere processes. Furthermore, as large amounts of sediments are entrained on the shallow Eurasian shelves during ice formation [*Eicken et al.,* 1997; *Dethleff et al.,* 1998], ice originating from the Laptev and East Siberian Seas largely determines the amount of sediment transport across the Arctic Ocean [*Nürnberg et al.,* 1994; *Pfirman et al.,* 1997].

Sea ice coverage and extent have routinely been monitored throughout the Arctic for some decades from space [*Gloersen et al.*, 1992]. These data sets and earlier ground-based and aerial observations [*Timokhov*, 1994; *Zakharov*, 1995] show that the Laptev Sea ice cover retreats by about 250,000 km^2 from mid-June to mid-September. In contrast, few data sets of ice thickness and its regional and temporal variability have been reported for this region [*Romanov,* 1993; *Timokhov,* 1994]. Thus, measurements of ice thickness at numerous Soviet drifting ice stations have been mostly limited to shorter profiles on individual floes [e.g., *Grishchenko*, 1976]. Large-scale surveys by upward looking sonars (ULS) onboard British or U.S. nuclear submarines are mostly confined to the western and central Arctic [*Bourke and McLaren,* 1992; *Wadhams,* 1994; *Rothrock et al.,* 1999].

In this paper we present results from extensive ground-based electromagnetic inductive (EM) and drill hole ice thickness profiling in the Laptev and northern Kara Seas and the adjacent sector of the central Arctic Ocean performed in August/September of 1993, 1995, and 1996. In 1996, more than 37 km of thickness profile data at 5 m horizontal spacing was acquired, partially extending over ice fields studied in 1995. This allows us to examine changes in ice thickness and morphology during the transition from first- to second-year ice.

The variability of the ice thickness distribution in the Laptev Sea is also of great interest in the context of recently observed decreases in sea level pressure in the central and Siberian Arctic [*Walsh et al.,* 1996] and associated changes in atmospheric circulation regimes. These resulted in decreases of summer ice extent, particularly in the Siberian Arctic, including the Laptev Sea [*Serreze et al.,* 1995; *Maslanik et al.,* 1996]. Our measurements coincide with three summers of intermediate (1993), record minimum (1995), and record maximum (1996) ice extent in the Laptev Sea (based on the period 1978-1998; see below). Thus differences in ice

Paper number 1999JC000088.
0148-0227/01/1999 JC000088$09.00

coverage, ice thickness, and extent of summer melt will be studied in relation to the prevailing summer atmospheric circulation. Furthermore, the data set may also help in validating large-scale sea-ice models during 2 extreme years in a region of prime importance for ice transport in the Transpolar Drift (TPD).

2. Location and Methods of Ice Thickness Measurements

2.1. Study Area and Measurements

Ice thickness measurements were carried out during three summer expeditions with the icebreaker R/V *Polarstern* in 1993, 1995, and 1996 [*Fütterer,* 1994; *Rachor,* 1997; *Augstein,* 1997]. All expeditions took place from late July to September (Table 1), extending from the end of the ablation season to fall freeze-up. Locations of the profiled ice floes are shown in Figures 1b-1e. Ice core and ice-rafted sediment data from the 1993 expedition have been published by *Eicken et al.* [1997]. In 1993 and 1995, measurements were confined to the Laptev and western East Siberian Sea, whereas in 1996 the northern Kara Sea and the central Arctic were also covered. The northernmost measurements of 1996 were obtained in an ice field that had been sampled in 1995, as shown by the trajectories of two Argos buoys deployed in 1995 (Figure 1f). This allowed for a Lagrangian study of ice thickness evolution. Furthermore, part of the 1996 study area in the central and eastern Laptev Sea coincided with that of 1995 (Figures 1c-1e).

Both drill hole and EM measurements were carried out in all 3 years along linear profiles with a point spacing of 4 or 5 m. In 1993 the measurements mainly served to validate the EM method along 100 m profiles [*Haas et al.,* 1997]. Here we only show drill hole results, which constitute the bulk of the data for this period. In 1995 and 1996, drill hole measurements were only made for validation purposes, and the majority of the data were derived with the EM technique (Table 1). The profile length ranged between 100 and 300 m (mean 180 m) in 1995. In 1996, 37 km of EM profiles were gathered on 35 floes, i.e., with a mean profile length of more than 1 km. These measurements covered the widest geographical area and extended northward to within 400 km of the North Pole. With the long profiles in 1995 and 1996, while the choice of floes was such as to include only those typical of the larger region with extensive level ice patches separated by ridges or ice rubble, no particular effort was made to avoid deformed ice or ridges on these floes. If possible, pressure ridges were crossed perpendicular to their longitudinal extension to reduce sampling bias in the occurrence of ridged ice probability.

From drill hole measurements, ice thickness (to within +/-3 cm), draft (to within +/-3 cm), and freeboard (to within +/-2 cm) as well as the thickness of the snow layer (to within +/-1 cm) or of the weathered surface ice layer (to within +/-1 cm) have been determined. The EM measurement technique and accuracy are described in more detail below. However, it is important to note here that EM sounding only yields the total ice thickness, i.e., the sum of ice plus snow or deteriorated surface layer thickness or the ice thickness plus meltwater depth in case of melt ponds. Therefore snow and deteriorated surface layer thickness or meltwater depth have to be measured independently to yield ice thickness, as has ice freeboard if it is of interest.

Here we determined the elevation of the ice or snow surface with a laser leveling device. Surveying was performed at 1 m intervals in 1995 along the entire thickness profiles. In 1996 these surface measurements (at a spacing of 5 m) comprised only 200-300 m at the start of each thickness profile. At the same locations the snow depth was determined with a ruler stick. In case melt ponds were present along the profiles, their extent and depth were determined with ruler stick and tape measure.

Figure 2 presents examples of typical thickness profiles measured in 1995 and 1996. In Figures 2a and 2b, melt ponds were located where the surface elevation was negative, with their water surface at sea level. EM draft was calculated by subtracting EM-derived ice thickness from surface height. In Figures 2c and 2d, the plotted draft and surface height beyond 200 m distance are virtual profiles, as they have been calculated only for illustration purposes from the EM-derived total thickness. A point-to-point isostatic equilibrium was assumed, and a mean draft-to-surface height ratio based on the drill hole measurements and survey results from the first 200 m of the profile was applied for plotting.

Because there was a considerable snow cover in 1996 (Figures 2c and 2d), the mean snow thickness in each identified ice regime (see below and Table 2) was subtracted from each single EM measurement to yield the ice thickness profile, which can then be compared with the measurements in 1993 and 1995 when no snow was present.

2.2. Background on EM Thickness Measurements

Ground-based EM measurements of sea ice thickness with a small portable instrument have been shown to yield reliable results [*Kovacs and Morey,* 1991]. In an earlier study [*Haas et al.,* 1997] we presented results of EM measurements in the

Table 1. Overview of Thickness Measurements[a]

Year	Region	Measurements	N_f[b]	N_{EM}/N_{drill}[b]	Total length, m
1993	Western Laptev Sea	drilling	12	0/510	1052
1995	Laptev Sea	EM/drilling	25	927/357	4510 (EM)
1996	Kara/Laptev Sea and central Arctic	EM/drilling	35	7500/312	37325 (EM)

[a] Compare with Figure 1.

[b] N_f is the number of floes sampled, and N_{EM} and N_{drill} are the number of EM and drill hole measurements, respectively

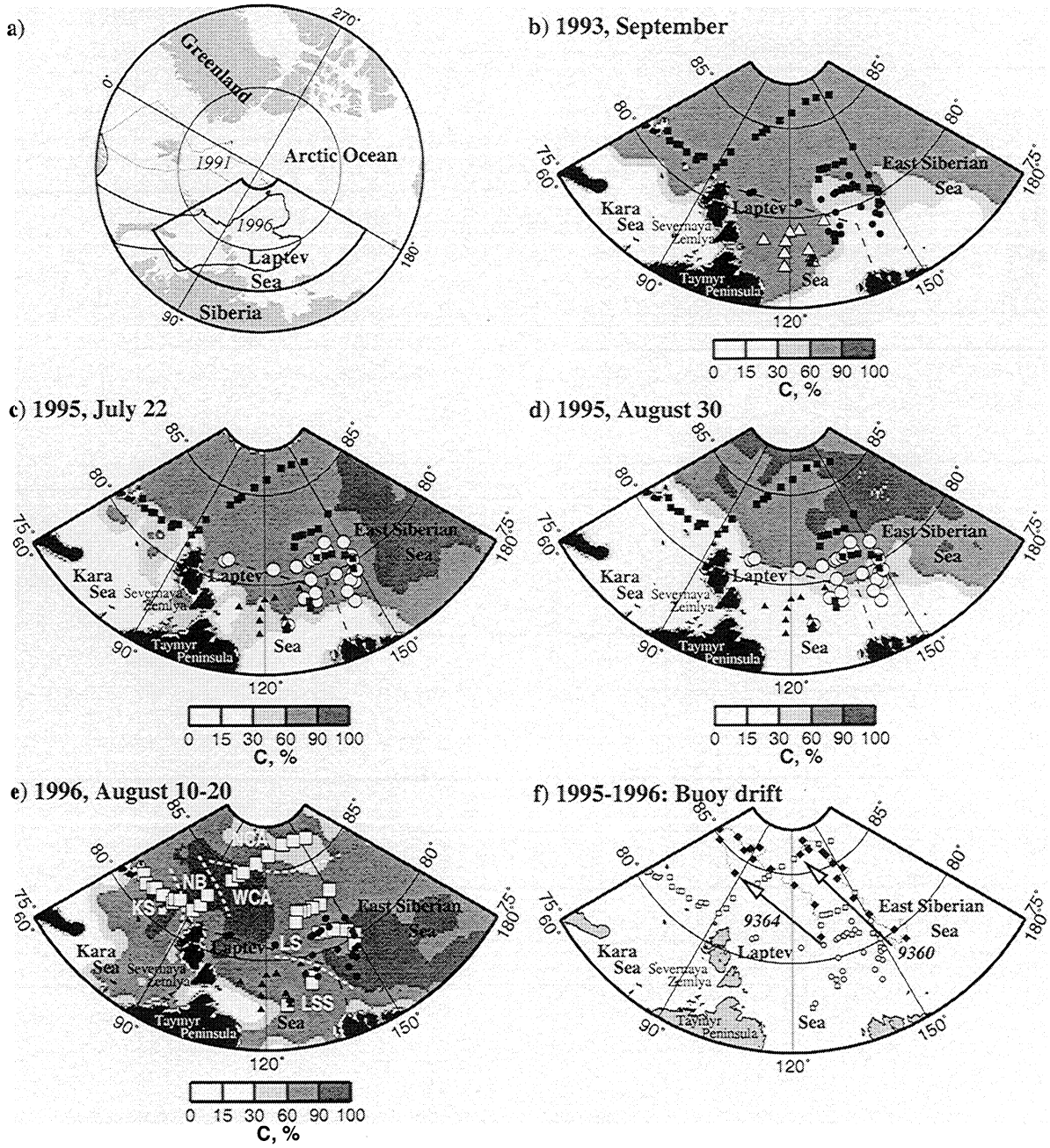

Figure 1. Maps of the study region showing the measurement locations (1993, triangles; 1995, circles; and 1996, squares): (a) Arctic Ocean with two cruise tracks of R/V *Polarstern* in *1991 [Eicken et al.*, 1995] and 1996. (b) – (e) Representative ice concentration maps for the summers of 1993 (mean ice coverage in September), 1995 (conditions at the beginning and end of measurements), and 1996 (mean for August 10-20) derived from satellite microwave data (Special Sensor Microwave Imager SSM/I); provided through Earth Observing System Data and Information System (EOSDIS), National Snow and Ice Data Center (NSIDC). The dashed line demarcates the Laptev Sea as defined by *Treshnikov* [1985], for which the time series of ice coverage was calculated (Figure 5). Six different subregions are identified in Figure 1e (see also Figures 7 and 8 and Tables 2 and 3). (f) Trajectories of two Argos buoys (ID 9360 and 9364) from September 1995 to August 1996. Black diamonds indicate the buoy locations at the first day of each month, starting in September 1995 and ending in August 1996 (arrows show total displacement).

Eurasian Arctic under extreme winter and summer conditions, demonstrating that the EM technique is applicable even in porous, ponded Arctic sea ice during summer melt.

EM induction measurements are performed by means of a low-frequency EM field (primary field), which is generated by a small transmitter coil. The EM field induces eddy currents in the saline, electrically conducting seawater with only a very small contribution from the low-conductivity ice. The eddy currents, in turn, generate a secondary EM field, which is detected by a receiver coil a few meters apart from the

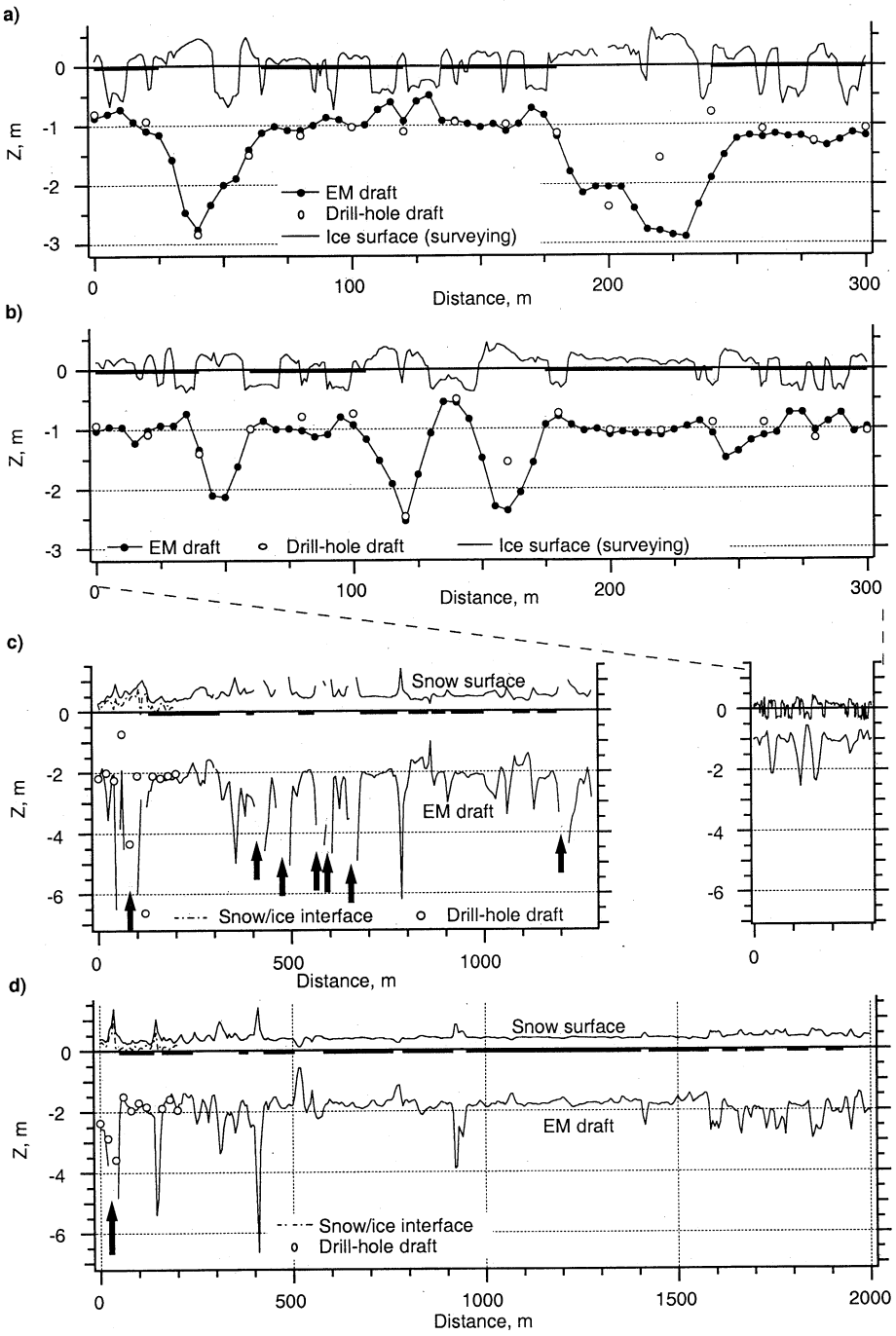

Figure 2. Typical profiles of ice draft and surface elevation, measured in (a) and (b) 1995 and (c) and (d) 1996 by means of EM sounding, drilling, and surveying. The arrows indicate very thick ice where the measured apparent conductivity was too small to be converted into ice thickness (see section 2.2). In Figures 2a and 2b, typical for the floes in the central Laptev Sea in 1995, negative surface elevation indicates the location of melt ponds whose water surface was at sea level. Figures 2c and 2d are typical for ice floes profiled in the northern and western central Arctic, respectively. In Figures 2a-2d the heavy horizontal lines at sea level identify level ice sections. For comparison, Figure 2b is also plotted next to Figure 2c at the same scale.

transmitter at the ice surface. The strength of the secondary field decreases with increasing distance between the coils and the ice-water interface. With the coils located at the ice or snow surface this distance is identical to the total ice and snow thickness.

Since the eddy currents are induced within an extended area of a few meters in diameter underneath the ice bottom and as the distance between the coils is finite and all conductors in the system are mutually coupled, ice thickness is always averaged over a footprint of some meters under the

Table 2. Mean and Modal Ice and Snow Thicknesses (± Their Standard Deviations) and Melt Pond Fractions Along the Thickness Profiles for All Data Sets From 1993 to 1996[a]

Year	Region	Approximate Location	N_f	Mean Ice Thickness, m	Standard Error, %	Mode, m (0.1 m bins)	Mean Snow Thickness, m	Melt Pond Fraction, %; Depth, m
1993 (Sept. 09-21)	Laptev Sea	-	11	1.85±0.78	29.4	1.75	-	-
1995 (July 22 to Sept. 04)	Laptev Sea (west)	-	8	2.15±1.23 (2.18±1.20[b])	34.2	1.45	0	22.8 / 0.27
	Laptev Sea (central)	-	8	1.38±0.80 (1.46±0.74[b])	27.0	1.15	0	29.4 / 0.33
	Laptev Sea (east)	-	9	1.99±1.12 (2.04±1.08[b])	44.9	1.35	0	22. / 0.22
	all	-	25	1.80±1.10 (1.86±1.05[b])	44.1	1.25	0	24.7 / 0.27
1996 (July 25 to Sept. 05)	Kara Sea (KS)	81°30'N, 67°-84°E	8	1.56±0.81	24.2	0.75	0.08±0.10	14.6
	Nansen Basin (NB)	81°45'-83°N, 91°30'E	3	2.27±1.12	33.8	1.45	0.07±0.09	0 (29.3[c])
	Western Central Arctic (WCA)	84°-85°30'N, 100°-113°E	3	2.06±0.57	3.8	1.85	0.21±0.16	0
	Northern Central Arctic (NCA)	85°30'-86°30'N, 121°-155°E	5	2.86±1.13	10.0	2.25	0.26±0.15	0
	Laptev Sea (LS)	83°-79°30'N, 130°-150°E	13	2.00±0.66	7.52	1.85	0.14±0.12	0
	Southern Laptev Sea (LSS)	78°50'-77°20'N, 133°-125°E	3	1.19±0.75	37.1	1.25/0.45	0.10±0.06	0

[a] The 1995 and 1996 data are subdivided into different ice regimes (see Figures 7 and 8). N_f is the number of floes studied in each region.
[b] Ice thickness plus meltwater depth.
[c] Saturated snow / slush.

instrument. Therefore small-scale variability or abrupt thickness changes appear smoothed in the EM data. In particular, the maximum depth of pressure ridges is generally underestimated because the water adjacent to the ridge keel also contributes to the secondary field [see also *Haas et al.*, 1997, Figure 4]. Furthermore, unconsolidated ridges with a high porosity cannot be sounded correctly. It has been demonstrated, however, that the mean thickness along a full pressure ridge cross profile can be determined to a sufficient accuracy [*Haas et al.*, 1997].

In this study all EM measurements were performed with a Geonics EM31 operated in horizontal magnetic dipole mode [*Haas et al.*, 1997]. The instrument has a signal frequency of 9.8 kHz and a coil spacing of 3.66 m. To shelter the instrument, to ease measurements over melt ponds, and to accelerate travel across the ice, the instrument was mounted in a polyethylene hull kayak, which was man-hauled along the profile, stopping every 5 m to take a reading.

The EM31 yields a reading of the apparent underground conductivity (in Millisiemens per meter, mS m^{-1}) which is directly proportional to the strength of the secondary field. While the relation between apparent conductivity and ice thickness is well known and can be numerically modeled [e.g., *Ward and Hohmann*, 1988], here a different approach to derive ice thickness from apparent conductivity was taken. For each measurement campaign, apparent conductivity was plotted against ice thickness measured at coincident points by drilling, and a least squares exponential fit was derived for the set of data points (Figure 3). By solving the resulting relations for ice thickness, transformation equations have been derived to convert apparent conductivity into ice thickness. These were then applied to all EM measurements of that particular measurement campaign. The advantage of this empirical approach is that no assumptions of ice or water conductivity have to be made. The different transformation equations for each year also take into account the prevailing level ice thickness. The thicker the level ice, the better the correspondence between the exponential fit and a one-dimensional (1-D) model curve at large thicknesses (Figure 3).

The good agreement between drill hole and EM derived thicknesses or drafts, is evident from the profiles shown in

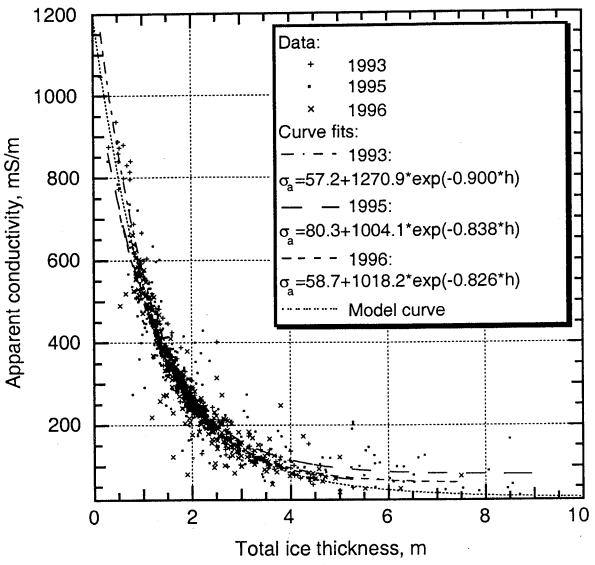

Figure 3. Measured apparent conductivity σ_a versus ice thickness h for all measurements and least squares exponential fits to these data. The equations that can be solved for ice thickness are also shown, as well as a 1-D two-layer model curve for level ice with a conductivity of 23 mS m^{-1} typical of summer sea ice [*Haas et al.*, 1997] over water of 2600 mS m^{-1}.

Figure 2. In Figure 4, thickness probability density functions (PDFs) derived from all coincident drill hole and EM measurements are shown for 1995 and 1996. The PDFs generally agree very well, with a slight underrepresentation of the thickest ice in the EM data. Modal thicknesses of the drill hole and EM-derived PDFs deviate by not more than 0.1 m, and the mean thicknesses agree within 6% of the drill hole data.

The described derivation of ice thicknesses fails, however, if apparent conductivities smaller than the constant first term in the equations in Figure 3 are measured over very thick deformed ice because then the argument of the logarithm of the transformation equation becomes negative. This was the case at all locations indicated by arrows in Figure2 2c and 2d. Inversion of EM cross sections of thick pressure ridges would ideally require 2-D conductivity modeling. Since only between 1.4 (in 1996) and 3% (in 1995) of the total data set consist of such low-conductivity measurements, they have been disregarded in the present study. In 1996 the majority of low-conductivity measurements (75) occurred in the northernmost sector of the study area (Figure 1e). In this region the derived mean thickness may thus be slightly too small.

Our empirical transformation equations are much better suited, however, for the derivation of thicknesses of moderately deformed ice than can be provided by a 1-D level ice model. On the basis of the relationships exemplified in Figure 3, soundings with the EM31 appear to yield reliable results for thicknesses of up to 6 m. Furthermore, as is obvious from the profiles in Figure 2, the technique allows for the determination of the amount of level and deformed ice.

3. Results

3.1. Ice Conditions in 1993, 1995, and 1996

Ice concentration maps for ice conditions representative of the study periods in the summers of 1993, 1995, and 1996 are shown in Figures 1b-1e, as derived from passive microwave Special Sensor Microwave Imager (SSM/I) data. The large interannual variability in the Laptev Sea summer minimum ice cover (obtained from the sum of all grid cells with ice concentrations >15%, with the boundaries as defined by *Treshnikov* [1985]; see Figures 1b-1e) is evident in Figure 5. In 1993, with a summer minimum cover close to the mean, ice extended south along the Taymyr Peninsula in the western Laptev Sea, while the eastern Laptev Sea and parts of the East Siberian Sea were ice-free as far north as 80°N (Figure 1b). In 1995 a record minimum ice extent occurred in the sector 80°-160°E (with a corresponding minimum in total Arctic ice extent [see also *Serreze et al.*, 1995; *Maslanik et al.*, 1996]. During August 1995 the ice edge rapidly retreated toward the north (Figures 1c and 1d), with almost the entire Laptev Sea, including the waters surrounding the Severnaya Zemlya archipelago, ice-free at the end of the month. Conditions in the East Siberian Sea were similar to those in 1993. In contrast, in 1996, almost the entire Laptev Sea remained ice-covered, resulting in a positive anomaly (the largest for the period 1987-1998), with only a small polynya extending east of Vilkitsky Strait and around the Lena Delta farther south (Figure 1e).

3.2. Overall Ice Thickness Distributions

Figure 6 shows modal and mean floe thicknesses as well as their standard deviations along the cruise track in 1996, from the Kara Sea, past the North Pole, and toward the Laptev Sea. On the basis of ice thickness and ice properties the profiled floes have been grouped into six different regional categories: Kara Sea (KS), Nansen Basin (NB), western and northern central Arctic (WCA and NCA), Laptev Sea (LS), and

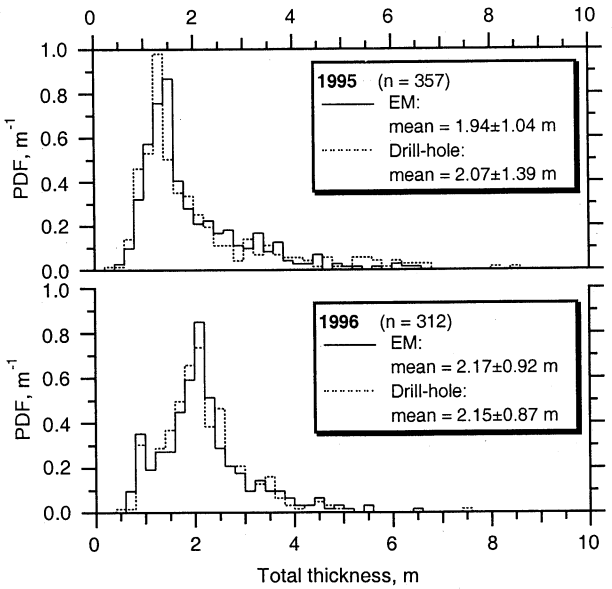

Figure 4. Comparison of ice thickness probability density functions (PDFs) derived by drilling and EM sounding at coincident points in 1995 and 1996.

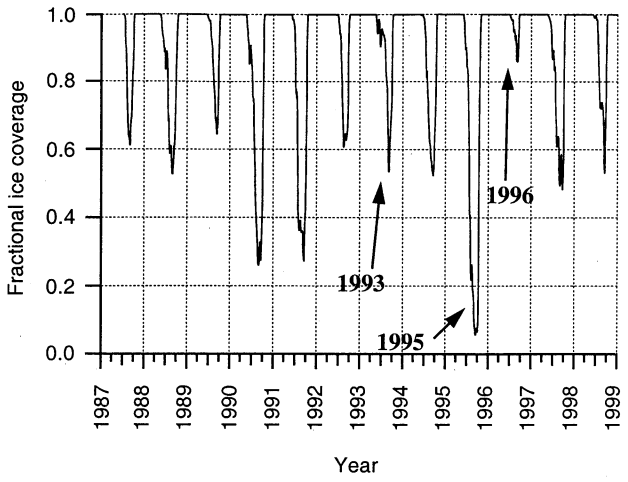

Figure 5. Fractional ice coverage (defined by 15% ice concentration contour) of the Laptev Sea derived from SSM/I passive microwave satellite data (provided through EOSDIS NSIDC).

southern Laptev Sea (LSS) (see also Figure 1e). Similarly, the 1995 measurements revealed three different ice regimes in the central, western, and eastern Laptev Sea, with the latter two having thicker ice mostly because of extensive deformation in the source areas [*Eicken et al.*, 2000]. Thickness PDFs for all measurements in 1993 and 1995 in the Laptev Sea as well as for each region identified in 1996 are presented in Figure 7 and summarized in Table 2. The southern Laptev Sea PDF was excluded from Figure 7c because its bimodal shape (cf. Figure 6 and Table 2) is highly biased by the positions of the sampled floes in relation to the ice edge of the polynya east off Taymyr Peninsula (see Figure 1e), where strong thickness gradients exist. A similar strong decrease of ice thickness close to the ice edge was observed in 1993 [*Eicken and Pac*, 1994] and is apparent from the small local maximum at 0.6 m in the 1993 PDF (Figure 7a).

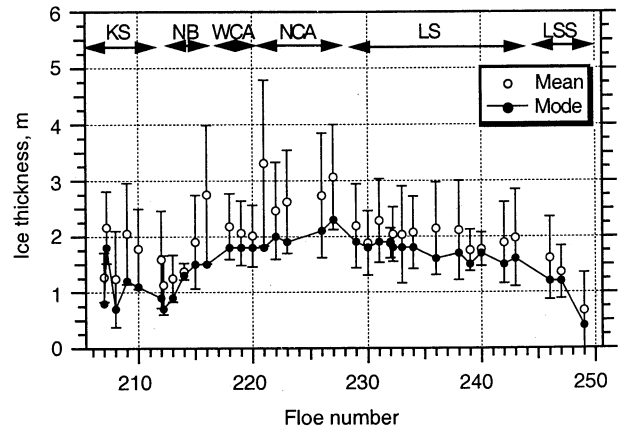

Figure 6. Mean and modal ice thickness of each floe sampled in 1996, along with their standard deviations (error bars). Arrows at the top indicate the subdivision of the cruise track into six different ice regimes: Kara Sea (KS), Nansen Basin (NB), western and northern central Arctic (WCA and NCA), Laptev Sea (LS), and southern Laptev Sea (LSS) (see also Figure 1e).

In 1995, mean ice thicknesses in the Laptev Sea ranged between 1.38 and 2.15 m. Typical thickness profiles of ponded ice in the central Laptev Sea are shown in Figures 2a and 2b. In 1996 the thinnest ice was found in the Kara Sea (mean 1.56 m) and the southern Laptev Sea (1.19 m), close to the ice edge (Table 2). In the Nansen Basin a gradual northward thickness increase was observed (Figure 6), with a mean value of 2.27 m and a mode of only 1.45 m (Table 2). Remarkably, the western central Arctic and the Laptev Sea had very similar thickness distributions, with mean values of 2.06 and 2.00 m, respectively. Only in the northern central Arctic,

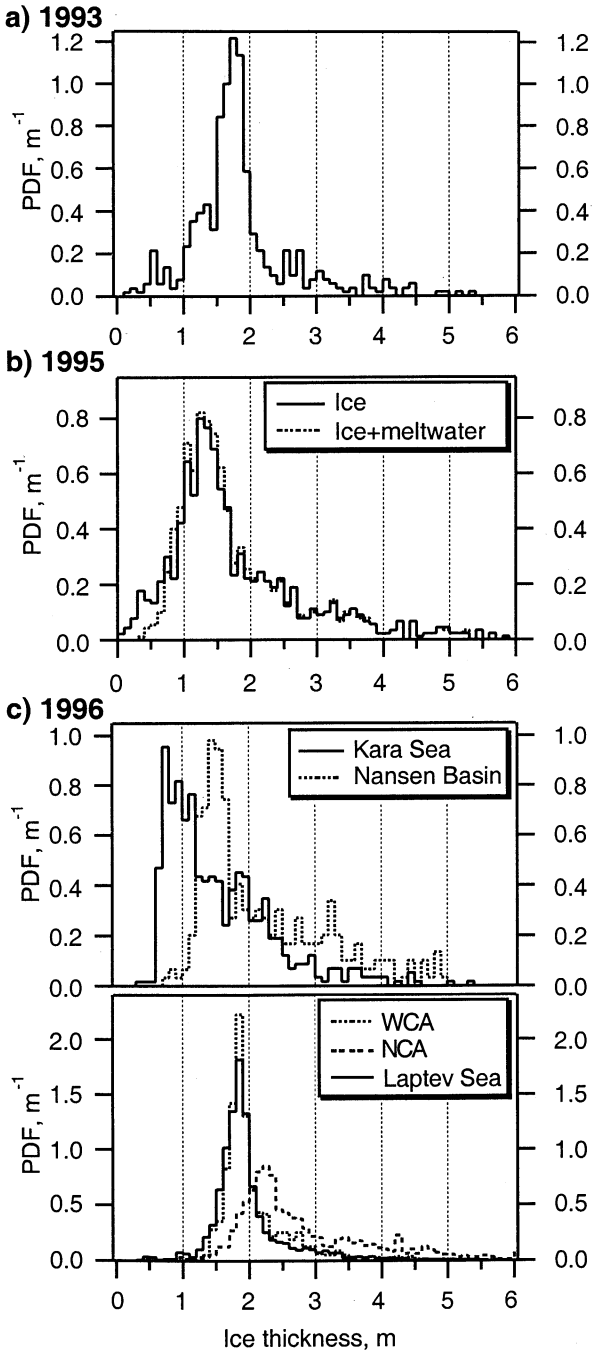

Figure 7. Ice thickness PDFs for all measurements in the Laptev Sea in (a) 1993 and (b) 1995, as well as for (c) each region in 1996 as defined from Figure 6.

higher ice thicknesses with a mean of 2.86 m were observed. The thickness profiles shown in Figures 2c and 2d are typical for the ice in the western and northern central Arctic, respectively.

Figure 7b includes a comparison of the ice thickness PDF and a PDF of ice thickness plus meltwater depth. As most ponds form over the thinnest level ice, the largest differences are apparent at modal and thinner ice thicknesses. The ice only PDF has a more pronounced tail at the low end owing to the extremely thin ice at the bottom of melt ponds (Figures 2a and 2b). For 1995, Table 2 lists both the mean ice and the mean ice plus meltwater thickness. The differences correspond to the mean pond depths, weighted by the melt pond fraction. Note that the standard deviation is higher for the mean ice thicknesses, indicating a roughening of the profiles by melt ponds (Figures 2a and 2b), which may persist into the winter season as suggested by *Buzuev and Spichkin* [1977]. The differences in ice thickness with and without melt ponds are important for comparisons with ULS data. The latter cannot distinguish between ponded and pond-free ice and will thus yield slight overestimates of the true summer thickness. The thinnest ice classes in ULS data are exclusively derived from young ice and not from thin ice at the bottom of ponds.

The ice regimes in 1996 differed largely in the degree of ice deformation, as can be seen from the standard deviations in Figure 6 and from the tails of the distributions in Figure 7c. Most notably, the ice in the western central Arctic and the Laptev Sea was little deformed, with a very narrow thickness distribution (cf. Figures 2c and. 2d). In 1995 the thickness distribution in the central Laptev Sea was similarly narrow, while heavily deformed and rubbled ice was observed in the western and eastern Laptev Sea.

To investigate whether the mean thicknesses given for the different regions differ significantly, we followed an approach by *Wadhams* [1997] in calculating the standard error ε of the mean thicknesses H in each region. The standard error $\varepsilon(L)$ as a function of profile length L is defined as

$$\varepsilon_H(L) = \left\{ \sum (H - H_i)^2 / n \right\}^{1/2},$$

with H_i the ith measured mean floe thickness of n floes. Here, L corresponds to mean profile lengths of 100, 180, and 1000 m for 1993, 1995, and 1996. In Table 2 the standard error is given as percentage of the mean. For most ice regimes, ε is greater than 20%, indicating that the differences between the means are not significant and that the regions do not represent very homogeneous ice fields. However, the standard errors of the modes (not shown here) are much smaller (see Figure 6), and the shapes of the PDFs differ considerably (Figure 7), such that distinguishing between the different ice regimes is generally justified. Significant differences in mean ice thickness are only found for the western and northern central Arctic and the Laptev Sea in 1996, with profiles long enough ($\geq$1 km) to yield representative thickness distributions.

Table 2 also summarizes melt pond and snow thickness data along the profiles. No values are given for 1993 because most ponds were already frozen and thin new snow covered the ice. Extensive surface melting also prevailed in 1995, with melt ponds and thaw holes covering up to 30% of the essentially bare and deteriorated ice surface. In contrast, in 1996 north of 84°N, melt ponds and slush were completely absent in the central Arctic and in the Laptev Sea except for a narrow zone close to the ice edge, where ponds were already frozen over in August. Instead, a highly metamorphosed snow cover had remained from the previous winter. Snow thickness increased from about 0.1 m in the southernmost regions to 0.26 m in the northern central Arctic. The mean density of 31 samples was 407±73 kg m^{-3}.

Melt pond fractions were highest in the central Laptev Sea in 1995, the region with the thinnest ice. In 1996 the transition between the melt pond-covered ice in the Kara Sea and the melt pond-free ice farther north extended through the Nansen Basin. While no ponds were apparent at the snow surface, the lower layers of the snow cover were slushy or even saturated with meltwater. The high fraction of 29.3% of this slush along the profiles shows how the snow retains the meltwater as no drainage system had yet developed.

A comparison of the thickness PDFs from 1993 and 1995 (Figures 7a and 7b) and from the Laptev Sea in 1996 (Figure 7c bottom) provides an overview of the interannual variability within the Laptev Sea (cf. Figures 1b-1e). The thickest ice was observed in 1996, but the mode was only 0.1 m higher than that of 1993 (Table 2). In 1995 the overall modal thicknesses were 1.25 and 1.15 m in the central Laptev Sea. This is 32 and 38% thinner than in 1996, respectively. The 1995 measurements were in the same range as the ice observed in the southern Laptev Sea in 1996.

3.3. Level Ice Thickness

Identification of level ice was based on one of two criteria. First, thickness variations along a level section were not allowed to exceed ±0.25 m. This criterion corresponds to that applied by, for example, *Melling and Riedel* [1995] or *Wadhams and Horne* [1980] to classify level segments in ice draft profiles. Second, following *Eicken et al.* [1995], a profile section was considered level when the local thickness did not depart by more than 50% from the mean at any point. While the former criterion is stronger for thicker ice, the latter is more restrictive for thinner ice. Generally, level sections had to be longer than 25 m, consisting of at least six measurement points. The level ice discrimination was based on bulk (ice plus meltwater) thicknesses, so as to distinguish between deformed and undeformed ice. Examples for level ice are illustrated in the profiles shown in Figure 2.

Table 3 lists the results derived from all data for the different regions identified above. Mean level ice thicknesses agree very well with the modes of the bulk thickness distributions (see Table 2), showing that the modes of the PDFs represent level ice. In all cases, level ice thicknesses are normally distributed (not shown here). The coefficients of variation, calculated for each level section and then averaged for Table 3, are indicators of the small-scale roughness of level ice. They were highest for the 1995 measurements, when the ice surface was extensively ponded (Figures 2a and 2b). In 1996 the lowest values were observed in the central Arctic and the Laptev Sea, where no signs of melt ponds were observed.

Level ice sections can be considered as being bounded by rough, deformed ice such as pressure ridges. Therefore the length of level sections and their relative proportion are measures of the degree of deformation and large-scale roughness of a floe. The mean values of these parameters are indicated in Table 3. The 1993 data have been omitted because of the short profile lengths. Note also that the 1995

Table 3. Characteristics of Level Ice.

Year	Region	Mean Amount of Level Ice, %	Mean Level Section Length, m	Mean Level Thickness, m	Mean Variation, %[a]
1993	Laptev Sea	-	-	1.64	8.8
1995	Laptev Sea (west)	51	55	1.53	12.9
	Laptev Sea (central)	71	77	1.20	16.0
	Laptev Sea (east)	54	46	1.45	11.3
1996	KS	68	66	1.24	12.9
	NB	47	65	1.59	11.2
	WCA	66	143	1.86	7.3
	NCA	50	78	2.23	7.5
	LS	62	107	1.78	5.6
	LSS	48	97	0.92	12.6

[a] Standard deviation divided by the mean for each level section

data may be biased by the rather short profile lengths of 180 m on average, which were mostly determined by the small floe size. Generally, these level ice data confirm that the least deformed ice was found in the central Laptev Sea in 1995 and in the western central Arctic and the Laptev Sea in 1996.

For the 1996 data, where the expedition covered the largest area, Figure 8 shows a correlation of mean level ice thickness H_l with latitude. Linear regressions for the sectors from the Kara Sea toward the North Pole (KS-NCA) and from the Laptev Sea toward the North Pole (LSS-NCA) yield the following relations:

KS- NCA

$$H_l\,[\mathrm{m}] = -17.6 + 0.23\ \mathrm{Lat\,[deg]},\quad 81.2°\mathrm{N} < \mathrm{Lat} < 86.5°\mathrm{N},\ r = 0.87$$

LSS- NCA

$$H_l\,[\mathrm{m}] = -11.7 + 0.16\ \mathrm{Lat\,[deg]},\quad 77.5°\mathrm{N} < \mathrm{Lat} < 86.5°,\ r = 0.92$$

with the correlation coefficient r. Thus the latitudinal thickness gradient is much steeper from the northern Kara Sea to the North Pole than from the Eastern Siberian Arctic. As surface melting was negligible in 1996, this is likely a result of smaller net freezing rates in the Kara Sea sector both because of higher ocean heat fluxes from inflowing Atlantic water and advection of warmer air masses from the North Atlantic. Interestingly, the gradient of 0.23 m deg^{-1} for level ice in the Kara Sea sector closely agrees with a gradient in mean draft of 0.22 m deg^{-1} derived from submarine ULS measurements along the prime meridian from 86° to 72°N in May 1987 [*Wadhams*, 1997], which is ascribed to a mixture of under-ice melt and mixing of ice types.

4. Discussion

4.1. Areal Integration of Ice Regimes From Satellite Radar Backscatter Data

Prior to discussing the interannual variability of ice thickness, ice conditions, and their dependence on atmospheric circulation patterns the developmental stage and age of the identified ice regimes have to be addressed in order to understand better the differences in the thickness distributions. Thus we distinguish first- (FY) and second-year (SY) ice as having experienced one or two winters, respectively (in accordance with *WMO* [1970]).

The interpretation is considerably advanced through analysis of ERS satellite radar backscatter data as shown in Figure 9, where backscatter maps are presented for the beginning of June 1993, 1995, and 1996. By this time, just prior to the onset of snow melt when the backscatter signal drops sharply, the backscatter coefficient is mainly controlled by the physical properties of the upper ice layers. In the Arctic, backscatter is generally higher for SY or multiyear (MY) ice than for FY ice owing to the higher number of scatterers and the lower dielectric loss factors for ice that has survived one or more melt seasons [*Onstott*, 1992; *Gohin et al.*, 1998; *Ezraty and Cavanie*, 1999]. In Figure 9c a pronounced gradient with increasing backscatter north of 85°N is evident. As the position of the buoys demarcates SY ice, the boundary between FY and SY ice is tentatively defined as the -16 dB isoline (dashed). Similarly, we have

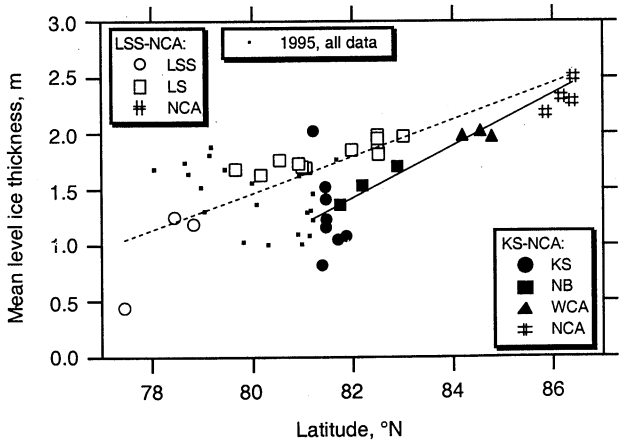

Figure 8. Mean level ice thickness versus latitude of all floes profiled in 1995 and 1996.

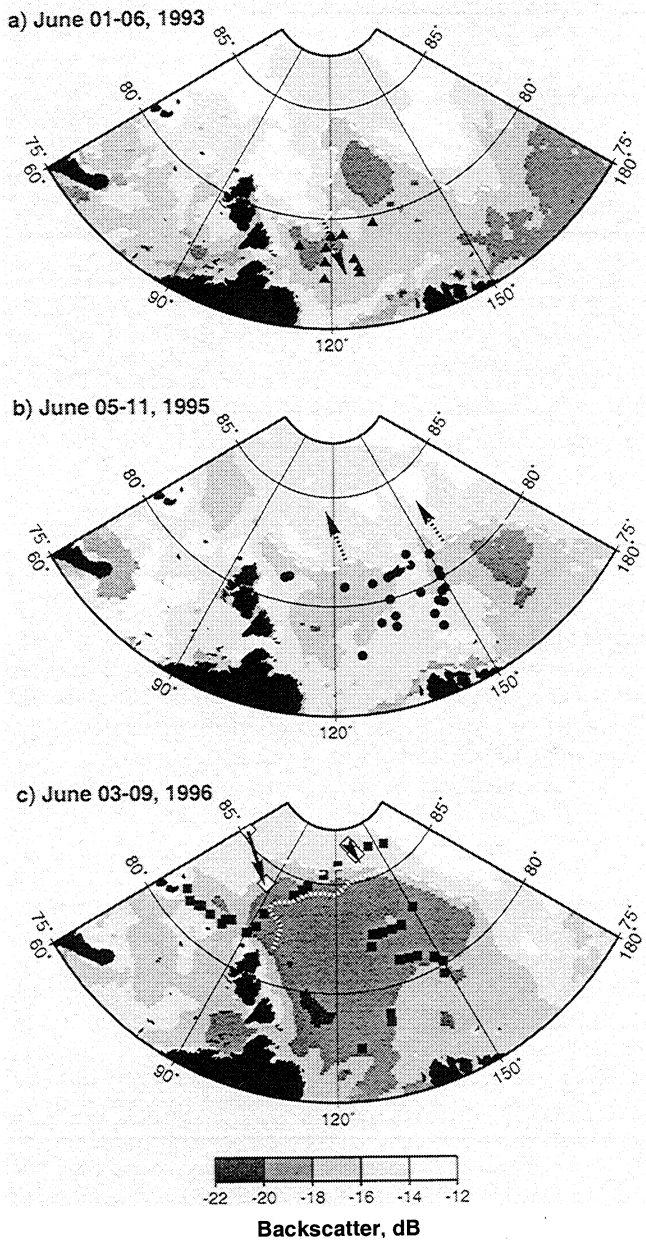

Figure 9. Maps of mean weekly radar backscatter from the ERS scatterometer at 40° incidence angle for the beginning of June (a) 1993, (b) 1995, and (c) 1996 (provided by CERSAT, IFREMER). Dashed lines indicate the FY (low backscatter) and SY (high backscatter) ice boundary. Solid triangles, circles, and squares show the locations of thickness measurements in August/September (see Figure 1). In Figures 9a and 9b, stippled arrows indicate the drift direction of the FY/SY boundary prior to sampling. In Figure 9c, the stippled line demarcates the reconstructed FY/SY boundary at the time of our measurementson the basis of the contemporaneous drift of two Argos buoys (open diamonds and arrows).

reconstructed the FY/SY boundary in 1993 and 1995 as the -16 dB isoline.

However, between the satellite images from early June and the thickness measurements in August/September the boundary had drifted quite some distance. In Figures 9a and 9b, the drift direction as deduced from sea level pressure fields (see Figure 10) is indicated by the stippled arrows. In Figure 9c the FY/SY boundary was reconstructed taking into account the buoy trajectories. Thus, in 1993 the ice had

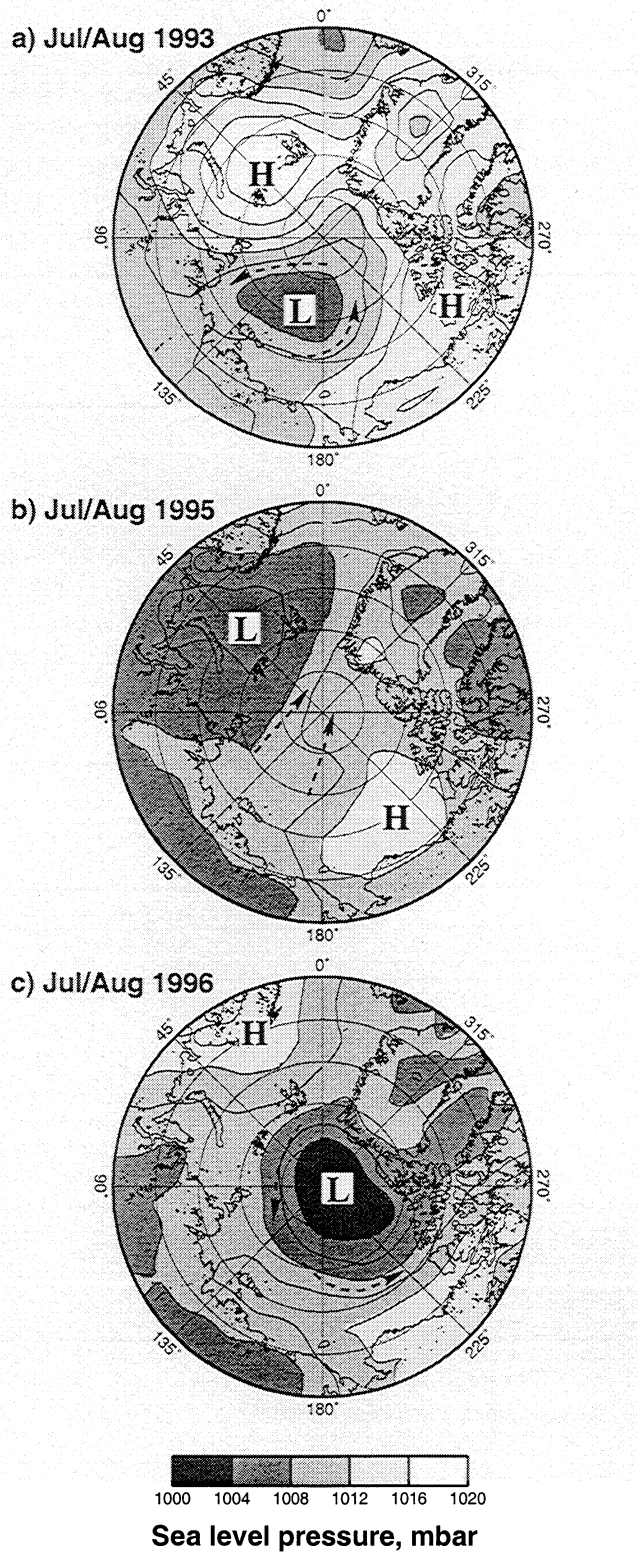

Figure 10. Mean sea level pressure in July and August (a) 1993, (b) 1995, and (c) 1996 (obtained from National Centers of Environmental Prediction (NCEP)/ National Center for Atmospheric Research (NCAR) reanalysis project).

recirculated into the Laptev Sea from farther north. As testified by Figure 9a and ice core studies, most floes were SY ice [*Eicken et al.*, 1997], constituting the so-called Taymyr Ice Massif east off the Severnaya Zemlya archipelago [*Barnett*, 1991]. The situation in 1993 corresponds to the long-term net southward drift in the western Laptev Sea [*Rigor and Colony*, 1997]. In 1995 the sampled ice consisted exclusively of FY ice (Figure 9b). For 1996, Figure 9c shows that the floes in the Kara Sea as well as in the Laptev and southern Laptev Seas were FY ice, and were SY ice in the northern central Arctic. However, the FY/SY boundary almost aligns with the sampling track in the Nansen Basin and western central Arctic. Given the small thickness of the ice in the Nansen Basin, this ice probably was of FY origin. The similarities in the ice thickness distributions between the western central Arctic and the Laptev Sea (Figure 7c, bottom) and studies of ice stratigraphy suggest FY ice for the former region as well. Most likely, the floes in the western central Arctic were located just along last summer's minimum ice edge (Figure 9c), and only some interspersed older ice occurred along the thickness profiles.

The FY ice radar backscatter shows large differences between 1993, 1995, and 1996 (Figure 9). As the data are from early June, the ice surface was not yet covered by melt ponds. Thus it is most likely that the backscatter contrasts result from the different geometric surface roughness, or amounts of deformed ice, as pressure ridges and ice rubble are stronger scatterers than smooth ice. As shown in Tables 2 and 3, the occurrence of the most level ice (western central Arctic and Laptev Sea in 1996) corresponds to a backscatter minimum (Figure 9c).

4.2. Interannual Variability in Relation to Variable Atmospheric Forcing

Our observations reveal significant interannual variability of summer conditions with respect to ice extent, ice drift, ice thickness, and surface ablation. This is explained in terms of different prevailing atmospheric circulation regimes presented in Figure 10 showing maps of the mean sea level pressure during July and August. These patterns control both the advection of ice and warm air.

As demonstrated by *Colony and Thorndike* [1984] and *Serreze et al.* [1989], during summer in the absence of significant internal ice stress the large-scale sea ice motion is driven by the geostrophic wind, with ice drift velocities amounting to about 1% of the wind speed at an angle of about 18° to the right of the wind. In 1993 a cyclonic pattern persisted north of the Laptev and East Siberian Seas (Figure 10a). As a consequence, ice was advected from the north into the western Laptev Sea, while it was removed from the east. This situation corresponds quite well to the mean annual ice velocity field given by *Rigor and Colony* [1997].

In July/August 1995, high air pressure dominated in the Beaufort Sea, while low pressure prevailed over the Kara and Barents Seas. The resulting southerly winds in the Laptev Sea region lead to northward ice drift and to the advection of warm air masses. The latter accelerated the northward ice retreat and caused the observed strong surface ablation and thin ice at the end of summer. In contrast, persistent cyclonic circulation around the central Arctic Basin dominated in 1996, leading to divergent, southward ice drift. As can be seen from the buoy trajectories in Figure 1f, the divergent, cyclonic motion commenced in June, when the northwestward drift reversed. The divergence results in ice concentrations of <60% north of 85°N visible in Figure 1e. In fact, on 2 days, visual ice observations revealed mean daily ice concentrations of <30% in this region [*Lensu and Haas*, 1998]. This circulation pattern also blocked the inflow of warm air into the Laptev Sea. The associated reductions in cloudiness and the downwelling longwave fluxes lead to the observed absence of surface melt and the persistence of a snow cover. The differences between 1995 and 1996 are also expressed in surface air temperatures obtained from the National Center for Environmental Prediction (NCEP), indicating a mean value of 0.90°C for July/August 1995 at 85°N, 120°E and of -0.14°C in 1996. Mean air temperatures in Tiksi and Cape Chelyuskin, two stations on the Laptev Sea coast, were 8.9° and 1.8°C from June to August 1995 and 3.5° and -0.6°C in 1996. In Tiksi the summer of 1995 was the warmest in the available record of 28 years, 2.4°C above average.

While the largest contribution to the presented pressure fields results from conditions in July, the mean pressure fields for June to August do not deviate significantly from those in Figure 10. Ice extent and thickness anomalies are particularly susceptible to variability in forcing during these 3 summer months. Our observations show that this annual summer variability is superimposed on a general trend of decreasing mean annual sea level pressure over the Arctic [*Walsh et al.* 1996] and over the Eurasian sector in particular [*Maslanik et al.*, 1996]. Also, during a general cyclonic Arctic Ocean surface circulation regime, as described by *Proshutinsky and Johnson* [1997] and *Proshutinsky et al.* [1999] for the period 1989-1997, the summer months might show reversed circulation patterns. Thus our results point to the importance of distinguishing between different seasons and timescales (seasonal, annual, and decadal) in assessing the variability of Arctic ice conditions. Therfore also linkages to planetary atmospheric waves, in particular the North Atlantic [e.g., *Hurrell*, 1995] and Arctic Oscillation [*Thompson and Wallace*, 1998] are not as pronounced since their forcing is weakest during the summer months [*Hurrell*, 1995].

The interannual variability is most distinct with respect to ice volume, i.e., the product of ice area and thickness. While the ice area in the Eurasian Arctic was strongly reduced in the summer of 1995 because of the extreme retreat of the ice edge, the volume reduction was even more pronounced because of substantial surface melt and concurrent reductions in ice thickness. In 1996, on the other hand, above average ice area and the widespread absence of surface melt and associated greater ice thickness resulted in the retainment of a high ice volume in the Siberian Arctic. In the northern central Arctic, however, the principally larger ice volume due to thicker ice was reduced by ice divergence and resulting low ice concentrations (Figure 1e). Nevertheless, it might still have been greater than in other years.

The present data set is spatially and temporally too sparse to allow for estimates of the seasonal and interannual variability in ice fluxes from the different sectors of the Eurasian Arctic. Likewise, the meridional ice thickness gradients characteristic of different age classes of ice grown in the Laptev Sea sector [*Rigor and Colony*, 1997] are not fully resolved and in part are overprinted by thickness changes due to strong gradients in ice ablation (see section 3.3).

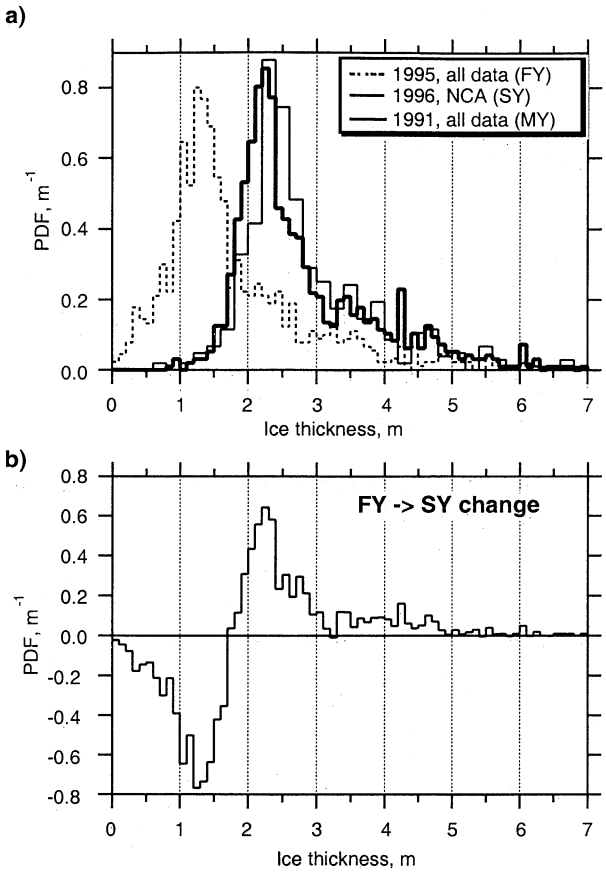

Figure 11. (a) Ice thickness PDFs of FY ice (1995), SY ice (1996), and level MY ice (1991) [*Eicken et al.*, 1995]. b) Thickness redistribution function derived for Lagrangian drift of ice field studied in 1995 and 1996.

Nevertheless, available buoy and satellite data as well as the atmospheric circulation patterns indicate that 1995 was a year of substantial summer ice export, while ice was imported into the Laptev Sea in the summers of 1993 (western half only) and 1996 (entire Laptev Sea).

The ice volume retained within the Laptev and East Siberian Seas has a large impact on the net freezing rate and associated salt and heat fluxes in autumn. Over the vast ice-free areas of 1995, about 2 m of level ice were grown in the subsequent winter. In contrast, the ice was already up to 1.85 m thick when freezing commenced in 1996, and thickening was most likely confined to a shorter time period and smaller net amount in the forthcoming winter season of 1996/1997. Thus variability in ice growth and salt fluxes conducive of deep water formation are most pronounced over the Siberian shelves.

It is interesting to note that the negative anomaly of 1995 in ice extent and volume did not propagate into the 1995/1996 ice season. In 1995, with anomalously high mixed layer heat content, fall freeze-up of the Laptev Sea was completed only on October 29, more than 2 weeks later than the climatological mean [*Eicken et al.*, 1997]. Nevertheless, thermodynamic growth and dynamic thickening were able to compensate for the ice volume anomaly, with a further promotion by highly reduced or absent surface melt in the summer of 1996. Mean and modal FY ice thicknesses of about 2 and 1.85 m, respectively, as found in the Laptev Sea and western central Arctic in 1996 (Table 2), agree well with mean estimates of *Rigor and Colony* [1997] based on a freezing degree days model by *Zubov* [1945]. If ice thicknesses were similar by the end of the winter 1994/1995, then the low modal ice thickness of 1.25 m found at the end of the melting season in 1995 suggests about 0.8 m of surface melting. This compares to a climatological mean of about 0.5 m [*Romanov*, 1993].

The ice thickness variability observed during this study, nevertheless, is still within the bounds of thickness variations measured in the North Pole region by submarine sonar since 1977 [*McLaren et al.*, 1994; *Shy and Walsh*, 1996] and emphasizes the difficulty involved in identifying trends or longer-term oscillatory patterns in ice thickness data. However, while the interannual variability in the submarine data is mostly assigned to ice dynamics and different ice origin or age, our data point to the importance of ablation processes on interannual variability as well, at least for measurements performed toward the end of the melt season, such as the draft measurements from the SCICEX submarine cruises [*Rothrock et al.*, 1999].

4.3. Ice Thickness Evolution in the Source Region of the TPD

On the basis of the conclusions from section 4.1. the 1995 data and the measurements in the northern central Arctic in 1996 reveal the changes in the ice thickness distribution (in a Lagrangian reference frame) of an ice field between its first and second summer season (Figure 11). The mean thickness increased from 1.80 m in 1995 to 2.86 m in 1996, while the modal ice thickness increased from 1.25 to 2.25 m in 1996 (Table 2). The tails of the 1995 and 1996 PDFs in Figure 11 indicate that the level ice thickness had not only increased but that this was accompanied by a similar increase in the thickness of deformed ice such that the overall shape of the PDF did not change significantly. Also, the fraction of level ice sections (Table 3) did not vary significantly (54 versus 50%), if the ice from the eastern Laptev Sea in 1995 is taken as the main source for the ice profiled in the northern central Arctic in 1996 as suggested by the drift of buoy 9360 (Figure 1f). In contrast, the mean level section length increased from 46 m in 1995 to 78 m in 1996. This might indicate the inclusion of newly formed level lead ice into the SY pack. More likely, however, this is due to leveling of rough ice as a result of ice growth during winter. As can be seen from the profiles in Figures 2b and 2c, the thickness of most of the deformed FY ice in 1995 hardly exceeded the level SY ice thickness in 1996. Thus the higher growth rates for thinner ice dampen or completely obliterate the amplitudes of bottom roughness elements and hence redistribute rough ice into level ice classes (Figure 11).

Figure 11a also shows the thickness distribution of level multiyear ice in the European sector of the central Arctic, i.e., downstream in the TPD. These data have been derived from drill hole measurements along 50 m profiles in 1991 between the North Pole and Svalbard (Figure 1a) [*Eicken et al.*, 1995] with a modal and mean thickness of 2.30 and 2.86+/-0.99 m, respectively. Notably, these values and the shape of the distribution are very similar to those derived for SY ice in the northern central Arctic in 1996 (Figure 11 and Table 2). The agreement between the means and the shapes of the

distributions may be just coincidental as the 1996 data consist of both level and deformed ice and level ice thickness alone was normally distributed rather than showing a pronounced tail. The similar modes, however, indicate that the SY ice exported from the Laptev Sea had almost reached equilibrium thickness [*Maykut and Untersteiner*, 1971] after two winters. In part, this is explained by the absence of significant surface melt during the summer of 1996. On the basis of climatological ablation data, net ice melt amounts to between 0.2 and 0.3 m [*Romanov*, 1993]. Therefore, in other years one would expect attainment of equilibrium thickness after three winters.

5. Conclusions

Thickness data from the Laptev Sea and the adjacent sector of the Arctic Ocean have been obtained in the summers of 1993, 1995, and 1996 from surveys employing an electromagnetic measurement technique. Comparison with drill hole data and modeling indicate that the accuracy of the EM measurements is better than 0.05-0.10 m and that the method is well suited for high-resolution thickness profiling. In particular, the ground-based studies enable a direct comparison between thickness data and surface characteristics such as melt pond coverage or surface albedo, which helps in the interpretation of ice thickness anomalies. In 1995 this comparison demonstrated the importance of melt ponds in determining small-scale roughness of the ice surface. Despite their limited extent the present data may provide an extension of the comprehensive submarine sonar ice draft data set obtained in recent years through the SCICEX program, which was limited to the deeper Arctic Basin [*Rothrock et al.*, 1999]. For future large-scale studies, airborne EM measurements in combination with laser altimetry hold considerable promise [*Kovacs and Holladay*, 1990; *Multala et al.*, 1996; *Haas*, 1998].

The importance and suitability of satellite radar scatterometer data for the areal integration of different ice regimes, as defined by their different thickness characteristics, was shown. In particular, the boundary between FY and SY ice could clearly be delineated. The study also demonstrated that the interpretation of radar data is greatly enhanced by taking into account the differences in geometric surface roughness derived for FY and SY ice. The ice thickness data compiled in this study allow delineation of different ice regimes in the Siberian Arctic, and through Lagrangian tracking, also provide information about the thickness evolution of an ice field exported from the Laptev Sea in 1995. Thus the below average FY ice thicknesses in 1995 had increased to values typical of SY and even MY ice. The distinct contrasts between the 1995 and 1996 melt seasons, with the former showing excessive ablation and the latter characterized by the near-complete absence of surface melt north of approximately 84°N, are linked to differences in the summer atmospheric circulation regime. In 1995 the advection of warm air from central Siberia can thus be considered to contribute significantly to the observed record minimum in Laptev Sea ice extent. As discussed also by, for example, *Maslanik et al.* [1996], it is difficult to separate such thermodynamic effects in explaining ice extent anomalies from dynamic components. In the present case, southerly winds also helped to compact and push the ice edge toward the North during late July and August of 1995. Similarly, the persistence of a pronounced low over the Arctic Basin in 1996 was responsible for increased divergence in the central Arctic and a southward displacement of the ice edge into the southern reaches of the Laptev Sea.

While the absence of surface melt may not be all that common in the present climatic regime, it is, nevertheless, of considerable importance in the context of negative surface freshwater flux anomalies observed in the Arctic Ocean [*B. Ekwurzel*, personal communication, 1999]. Moreover, during periods of reduced surface heat fluxes, such events may be more widespread, with pronounced effects on surface albedo. Currently, large-scale sea ice models may have difficulties in properly representing the summer albedo evolution (which does not change significantly from the winter value in the absence of melt) as the albedo is commonly parameterized as a function of surface temperature. Surface temperatures derived from the NCEP reanalysis data for the 2 years studied here indicate comparatively small deviations in surface temperatures, however.

Most important, the present study demonstrates the considerable interannual variability in ice thickness in a region with the highest net ice accretion rates throughout the interior Arctic. In part, this variability is due to recirculation and enhanced deformation of ice over the shelf (such as was observed in 1993), which may result in level ice thicknesses in excess of 1.5-2 m exiting into the Transpolar Drift. As demonstrated by the thickness distribution of SY and MY ice, level ice in the interior Arctic is likely to attain its equilibrium thickness well before exiting through Fram Strait [*Maykut and Untersteiner*, 1971]. This underscores the importance of growth and deformation of new ice in leads as compared to level ice anomalies in determining the ice mass flux through Fram Strait. The other factor contributing to variability in ice thickness is surface melt, which has been shown to vary considerably in subsequent years. These differences are particularly important for the evolution of surface albedo and the amount of shortwave energy supplied to the ice cover and the upper ocean. Their impact on the mass balance of level ice farther downstream in the TPD is not likely to be as pronounced since enhanced thickening of thinner ice during the subsequent winter (such as was observed in 1996) tends to dampen such thickness anomalies.

Acknowledgments. We are most grateful to all who helped the drilling and kayak hauling in the field, particularly to Mikko Lensu and Till Scherzinger. This study would not have been possible without the support of cruise leaders and crew of R/V *Polarstern*. SSM/I passive microwave data were obtained on CD-ROM from the EOSDIS NSIDC Distributed Active Archive Center, University of Colorado, Boulder. Sea level pressure fields were provided by the NCEP/NCAR reanalysis project through the NOAA Climate Diagnostics Center (http://www.cdc.noaa.gov). We obtained ERS scatterometer data ("Polar Sea Ice Grids") from CERSAT at IFREMER (http://www.ifremer.fr/cersat). Part of this study was supported by grants from the German Ministry of Research BMBF.

References

Augstein, E., The expedition ARCTIC '96 of RV "Polarstern" (ARK XII) with the Arctic Climate System Study (ACSYS), *Rep. Polar Res.*, *234*, 54 pp., 1997.

Barnett, D., Sea ice distribution in the Soviet Arctic, in *The Soviet Maritime Arctic*, edited by L.W. Brigham, pp. 47-62, Belhaven, London, 1991.

Bourke, R. H., and A. S. McLaren, Contour mapping of Arctic Basin ice draft and roughness parameters, *J. Geophys. Res.*, *97*, 17,715-17,728, 1992.

Buzuev, A. Y., and V. A. Spichkin, Influences of puddles on the spatial nonuniformity of thickness of multi-year ice in winter (in Russian), *Probl. Arktik. Antarktik.*, *49*, 53-58, 1977.

Colony, R., and A. S. Thorndike, An estimate of the mean field of Arctic sea ice motion, *J. Geophys. Res.*, *89*, 10,623-10,629, 1984.

Dethleff, D., P. Loewe, and E. Kleine, The Laptev Sea flaw lead: Detailed investigation on ice formation and export during 1991/1992 winter season, *Cold Reg. Sci. Technol.*, *27*, 225-243, 1998.

Eicken, H., and R. Pac, Thickness, structure and properties of sea ice, in *The Expedition ARCTIC '93, Leg ARK-IX/4 of RV "Polarstern" 1993*, edited by D. K. Fütterer, *Rep. Polar Res.*, *149*, 51-55, 1994.

Eicken, H., M. Lensu, M. Leppäranta, W. B. Tucker, A. J. Gow, and O. Salmela, Thickness, structure and properties of level summer multi-year ice in the Eurasian sector of the Arctic Ocean, *J. Geophys. Res.*, *100*, 22,697-22,710, 1995.

Eicken, H., E. Reimnitz, V. Alexandrov, T. Martin, H. Kassens, and T. Viehoff, Sea-ice processes in the Laptev Sea and their importance for sediment export, *Cont. Shelf Res.*, *17*, 205-233, 1997.

Eicken, H., J. Kolatschek, J. Freitag, F. Lindemann, H. Kassens, and I. Dmitrenko, A key source area and constraints on entrainment for basin-scale sediment transport by Arctic sea ice, *Geophys. Res. Lett.*, *27*, 1919-1922, 2000.

Ezraty, R., and A. Cavanie, Intercomparison of backscatter maps over Arctic sea ice from NSCAT and the ERS scatterometer, *J. Geophys. Res.*, *104*, 11,471-11,483, 1999.

Fütterer, D. K., The expedition ARCTIC '93, Leg ARK-IX/4 of RV "Polarstern" 1993, *Rep. Polar Res.*, *149*, 1994.

Gloersen, P., W. J. Campbell, D. J. Cavalieri, J. C. Comiso, C. L. Parkinson, and H. J. Zwally, Arctic and Antarctic sea ice, 1978-1987: Satellite passive-microwave observations and analysis, *NASA Spec. Publ., SP-511*, 290 pp. 1992.

Gohin, F., A. Cavanie, and R. Ezraty, Evolution of the passive and active microwave signatures of a large sea ice feature during its 2 1/2-year drift through the Arctic Ocean, *J. Geophys. Res.*, *103*, 8177-8189, 1998.

Gordienko, P. A., Arctic ice drift, in *Proceedings on the Conference on Arctic Sea Ice*, edited by R. W. Thurston, pp. 210-222, Natl. Res. Counc., Natl. Acad. of Sci., Washington, D.C., 1958.

Grishchenko, V. D., Statistical characteristics of several parameters of the relief of the upper and lower surface of drifting ice (in Russian), *TR. Arkt. Antarkt. Nauchno Issled. Inst., 320,* 214-221, 1976.

Haas, C., Evaluation of ship-based electromagnetic-inductive thickness measurements of summer sea-ice in the Bellingshausen and Amundsen Sea, *Cold Reg. Sci. Technol.*, *27*, 1-16, 1998.

Haas, C., S. Gerland, H. Eicken, and H. Miller, Comparison of sea-ice thickness measurements under summer and winter conditions in the Arctic using a small electromagnetic induction device, *Geophysics*, *62*, 749-757, 1997.

Harder, M., P. Lemke, and M. Hilmer, Simulation of sea ice transport through Fram Strait: Natural variability and sensitivity to forcing, *J. Geophys. Res.*, *103*, 5595-5606, 1998.

Hurrell, J. W., Decadal trends in the North Atlantic Oscillation regional temperatures and precipitation, *Science*, *269*, 676-679, 1995.

Kovacs, A., and J. S. Holladay, Sea-ice thickness measurements using a small airborne electromagnetic sounding system, *Geophysics*, *55*, 1327-1337, 1990.

Kovacs, A., and R. M. Morey, Sounding sea-ice thickness using a portable electromagnetic induction instrument, *Geophysics*, *56*, 1992-1998, 1991.

Lensu, M., and C. Haas, Comparison of ice thickness from ship based video and field data, in *Ice in Surface Waters*, edited by H. T. Shen, pp. 225-230, A. A. Balkema, Brookfield, Vt., 1998.

Maslanik, J. A., M. C. Serreze, and R. G. Barry, Recent decreases in Arctic summer ice cover and linkages to atmospheric circulation anomalies, *Geophys. Res. Lett.*, *23*, 1677-1680, 1996.

Maykut, G. A., and N. Untersteiner, Some results from a time-dependent thermodynamic model of sea ice, *J. Geophys. Res.*, *76*, 1550-1575, 1971.

McLaren, A. S., R. H. Bourke, J. E. Walsh, and R. L. Weaver, Variability in sea-ice thickness over the North Pole from 1958 to 1992, in *The Polar Oceans and Their Role in Shaping the Global Environment*, *Geophys. Monogr. Ser.*, vol. 85, edited by O. M. Johanessen, R. D. Muench, and J. E. Overland, pp. 363-371, AGU, Washington, D. C., 1994.

Melling, H., and D. A. Riedel, The underside topography of sea ice over the continental shelf of the Beaufort Sea in the winter of 1990, *J. Geophys. Res.*, *100*, 13,641-13,653, 1995.

Multala, J., H. Hautaniemi, M. Oksama, M. Leppäranta, J. Haapala, A. Herlevi, K. Riska, and M. Lensu, An airborne electromagnetic system on a fixed wing aircraft for sea ice thickness mapping, *Cold Reg. Sci. Technol.*, *24*, 355-373, 1996.

Nürnberg, D., I. Wollenburg, D. Dethleff, H. Eicken, H. Kassens, T. Letzig, E. Reimnitz, and J. Thiede, Sediments in Arctic sea ice: Implications for entrainment, transport and release, *Mar. Geol.*, *119*, 185-214, 1994.

Onstott, R. G., SAR and scatterometer signatures of sea ice, in *Microwave Remote Sensing of Sea Ice*, *Geophys. Monogr. Ser.*, vol. 68, edited by F.D. Carsey, pp. 73-104, AGU,Washington, D. C., 1992.

Pfirman, S. L., R. Colony, D. Nürnberg, H. Eicken, and I. Rigor, Reconstructing the origin and trajectory of drifting Arctic sea ice, *J. Geophys. Res.*, *102*, 12,575-12,586, 1997.

Proshutinsky, A. Y., and M. A. Johnson, Two circulation regimes of the wind-driven Arctic Ocean, *J. Geophys. Res.*, *102*, 12,493-12,514, 1997.

Proshutinsky, A. Y., I. V. Polyakov, and M. A. Johnson, Climate states and variability of Arctic ice and water dynamics during 1946-1997, *Polar Res.*, *18*, 135-142, 1999.

Rachor, E., Scientific cruise report of the Arctic expedition ARK-XI/1 of RV "Polarstern" in 1995, *Rep. Polar Res.*, *226*, 157 pp., 1997.

Rigor, I., and R. Colony, Sea-ice production and transport of pollutants in the Laptev Sea, 1979-1993, *Sci. Total Environ.*, *202*, 89-110, 1997.

Romanov, I. P., *Ice Cover of the Arctic Basin*, I. P. Romanov, St. Petersburg, 192 pp., 1993.

Rothrock, D. A., Y. Y., and G. A. Maykut, Thinning of the Arctic sea-ice cover, *Geophys. Res. Lett.*, *26*, 3469-3472, 1999.

Serreze, M. C., A. S. McLaren, and R. G. Barry, Seasonal variations of sea ice motion in the Transpolar Drift Stream, *Geophys. Res. Lett.*, *16*, 811-814, 1989.

Serreze, M. C., J. A. Maslanik, J. R. Key, and R. F. Kokaly, Diagnosis of the record minimum in Arctic sea ice area during 1990 and associated snow cover extremes, *Geophys. Res. Lett.*, *22*, 2183-2186, 1995.

Shy, T. L., and J. E. Walsh, North Pole ice thickness and association with ice motion history 1977-1992, *Geophys. Res. Lett.*, *23*, 2975-2978, 1996.

Thompson, D. W. J., and J. M. Wallace, The Arctic Oscillation signature in the wintertime geopotential height and temperature fields, *Geophys. Res. Lett.*, *25*, 1297-1300, 1998.

Timokhov, L. A., Regional characteristics of the Laptev and the East Siberian Seas: Climate, topography, ice phases, thermohaline regime, and circulation, *Rep. Polar Res.*, *144*, 15-31, 1994.

Treshnikov, L. A., *Arctic Atlas* (in Russian), 204 pp., Main Dep. of Geod. and Cartogr. Under the Counc. of Minist. of the USSR, Moscow, 1985.

Wadhams, P., Sea ice thickness changes and their relation to climate, in *The Polar Oceans and Their Role in Shaping the Global Environment*, *Geophys. Monogr. Ser.*, vol. 85, edited by O. M. Johanessen, R. D. Muench, and J. E. Overland, pp. 337-362, AGU, Washington, D. C., 1994.

Wadhams, P., Ice thickness in the Arctic Ocean: The statistical reliability of experimental data, *J. Geophys. Res.*, *102*, 27,951-27,959, 1997.

Wadhams, P., and R. J. Horne, An analysis of ice profiles obtained by submarine sonar in the Beaufort Sea, *J. Glaciol.*, *25*, 401-424, 1980.

Walsh, J. E., W. L. Chapman, and T. L. Shy, Recent decrease of sea level pressure in the central Arctic, *J. Clim.*, *9*, 480-486, 1996.

Ward, S. H., and G. W. Hohmann, Electromagnetic theory for geophysical applications, in *Electromagnetic Methods in Applied Geophysics*, vol. 1, *Theory, SEG Monogr.*, vol. 3, edited by M. N. Nabighian, pp. 131-313, Soc. of Explor. Geophys., Tulsa, Okla., 1988.

World Meteorological Organization (WMO), WMO sea-ice nomenclature, terminology, codes, and illustrated glossary, *WMO/OMM/BMO 259*, 147 pp., Sec. of the World Meteorol. Org., Geneva, 1970.

Zakharov, V. F., *Sea Ice in the Climate System* (in Russian), Gidrometeoizdat, St. Petersburg, Russia, 15-26, 1995.

Zubov, N. N., *Arctic Ice*, 491 pp., Moscow, Russia, 1945. (English translation, U. S. Air Force Geophys. Lab., Techn. Rep., *79-34*, 500 pp., 1979.)

H. Eicken, Geophysical Institute, University of Alaska, 903 Koyukuk Dr., P.O. Box 757320, Fairbanks, AK99775-7320. (hajo.eicken@gi.alaska.edu)

C. Haas, Alfred Wegener Institute for Polar and Marine Research, Bussestrasse 24, D-27570 Bremerhaven, Germany. (chaas@awi-bremerhaven.de)

(Received October 8, 1999; revised August 10, 2000;
accepted October 6, 2000.)